

Debiased Sample Selection for Combating Noisy Labels

Qi Wei¹, Lei Feng^{1*}, Haobo Wang², Bo An¹

¹School of Computer Science and Engineering, Nanyang Technological University, Singapore

²School of Software, Zhejiang University, China

{qi.wei, lei.feng, boan}@ntu.edu.sg, wanghaobo@zju.edu.cn

Abstract

Learning with noisy labels aims to ensure model generalization given a label-corrupted training set. The sample selection strategy achieves promising performance by selecting a label-reliable subset for model training. In this paper, we empirically reveal that existing sample selection methods suffer from both data and training bias that are represented as imbalanced selected sets and accumulation errors in practice, respectively. However, only the training bias was handled in previous studies. To address this limitation, we propose a noIse-Tolerant Expert Model (ITEM) for debiased learning in sample selection. Specifically, to mitigate the training bias, we design a robust network architecture that integrates with multiple experts. Compared with the prevailing double-branch network, our network exhibits better performance of selection and prediction by ensembling these experts while training with fewer parameters. Meanwhile, to mitigate the data bias, we propose a mixed sampling strategy based on two weight-based data samplers. By training on the mixture of two class-discriminative mini-batches, the model mitigates the effect of the imbalanced training set while avoiding sparse representations that are easily caused by sampling strategies. Extensive experiments and analyses demonstrate the effectiveness of ITEM. Our code is available at this url [ITEM](#).

1 Introduction

The remarkable generalization capability of deep neural networks (DNNs) is achieved through training on a large-scale dataset [1, 2]. However, existing training sets are usually collected by online queries [3], crowdsourcing [4], and manual annotations, which could inevitably incur wrong (or noisy) labels [5]. Since DNNs exhibit vulnerability to such low-quality datasets [6], training on the label-corrupted set presents a great challenge for modern DNNs. Therefore, to investigate learning with noisy labels (LNL) [5, 7, 8, 9] is practically important, which contributes to improvements of model’s generalization on real-world applications.

Sample selection [10, 11, 12], a prevailing strategy for LNL, achieves considerable performance in mitigating the effects of noisy labels [13] by carefully selecting clean samples from the label-corrupted training set. The performance of sample selection approaches is largely decided by the selection criteria, which can be roughly categorized into two sides: 1) *small-loss* based strategies [8, 10, 12, 14, 15, 16], which are motivated by the memorization effect [17] that DNNs learn simple patterns shared by majority examples before fitting the noise. Hence, the samples with small losses in the early learning stage can normally be taken as clean samples. 2) *fluctuation* based strategies [9, 11, 18, 19], which are motivated by the observation that DNNs easily give inconsistent prediction results for noisy samples [11]. These methods normally consider an instance incorrectly labeled if its prediction results exhibit alterations within two consecutive training rounds or during a specified subsequent period.

Despite the validated effectiveness, there is a common view shared by existing sample selection methods that the sample selection processes are only influenced by a training bias, i.e., the accumulated error. In this paper, we for the first time show that by extensive experiments there exists another type of bias, i.e., the *data bias*, which is mainly caused by imbalanced data distribution. To be concrete, we split the bias in a selection-based learning framework into the training bias, which inherently exists in a self-training manner, and the data bias, which indicates the selected set tends to be class-imbalanced (see Figure 1). Therefore, the model is usually trained on class-imbalanced biased sets, resulting in sub-optimal results. Meanwhile, our experiments also provide some nontrivial findings, including 1) *a corrupted selection tendency* (see Figure 2a). The manner of self-training would exacerbate the imbalanced ratio in

* corresponding author

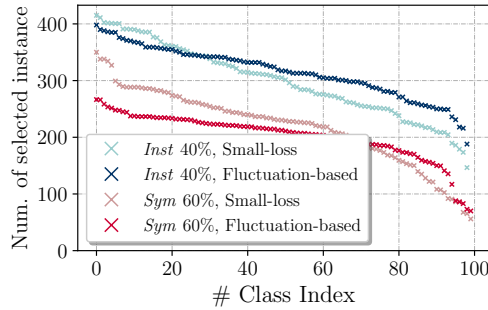


Figure 1: **Existing selection criteria always lead to the imbalanced training set.** We train ResNet-18 on noisy CIFAR-100 with two common selection strategies, including small-loss selection [10] and fluctuation-based noise filtering [11]. Class-level selected samples in the last epoch are counted.

the training process. 2) *class-discriminative selection performance* (see Figure 2b). Although the overall selection performance is gradually improved as the training process proceeds, the performance on tail classes exhibits obvious degeneration. The above observations motivate us to consider a novel learning framework that can simultaneously deal with both training bias and data bias.

To this end, we propose a noise-Tolerant Expert Model (ITEM), consisting of a noise-robust multi-experts structure and a mixed sampling strategy. Firstly, motivated by the idea of ensemble learning [20, 21], we design a robust network architecture that integrates the classifier with multiple experts to mitigate the training bias. Specifically, compared with the prevailing double-branch network [10, 12] where one network feeds selected samples to the other network, we independently conduct classifier learning and sample selection on different output layers. Therefore, incorrect selection results yielded by expert layers would not directly degenerate the classifier in subsequent learning, mitigating the accumulated error to a large degree. Meanwhile, compared with the double-branch network, our network is resource-friendly thanks to fewer trainable parameters and achieves better performance by combining multiple experts. Secondly, to confront the data bias, we propose a mixed sampling training strategy based on weighted data sampling. By calculating the quantity per class in the selected set, we obtain weights of different classes and further reverse weights via a mapping function for assigning larger weights to tail classes when sampling. Eventually, by using the mixup operation [22], our network is trained on a mixed mini-batch that combines two mini-batches respectively yielded by these two weighted samplers. This strategy fulfills class-balanced learning while avoiding sparse representations caused by the sampling strategy.

Our contribution can be summarized as follows:

- We propose a noise-robust network architecture. Our multi-experts network is resource-friendly and exhibits improved robustness compared with the double-branch network. It shows significant potential in becoming the backbone to tackle noisy labels.
- We propose a mixed sampling strategy, enabling the model to learn from tail classes via weighted samplers while avoiding sparse representations.
- ITEM achieves significant performance on both synthetic and real-world noisy datasets, ensuring the effectiveness of our proposal on practical applications.

We also provide abundant analyses, verifying the effectiveness of each component in ITEM.

2 Related Work

Sample selection for LNL. Previous sample selection methods normally exploit the memorization effect of DNNs, i.e., DNNs first memorize training data with clean labels and then those with noisy labels [10, 23]. The small-loss criterion [10] is a typical method stemming from the memorization effect, which splits the noisy training set via a loss threshold. The samples with small losses are regarded as clean samples. Moreover, some researchers modified the small-loss criterion and proposed to select by leveraging the idea of disagreement [14], a regularization term (the Jensen-Shannon Divergence) [8], and a Mixture Gaussian Model for fitting the loss distribution [12], respectively. Besides, to mitigate the accumulated error caused by sample selection, current methods always resort to a double-branch network structure that ensembles selection results from two networks [8, 10, 12, 14, 24]. Besides, some studies

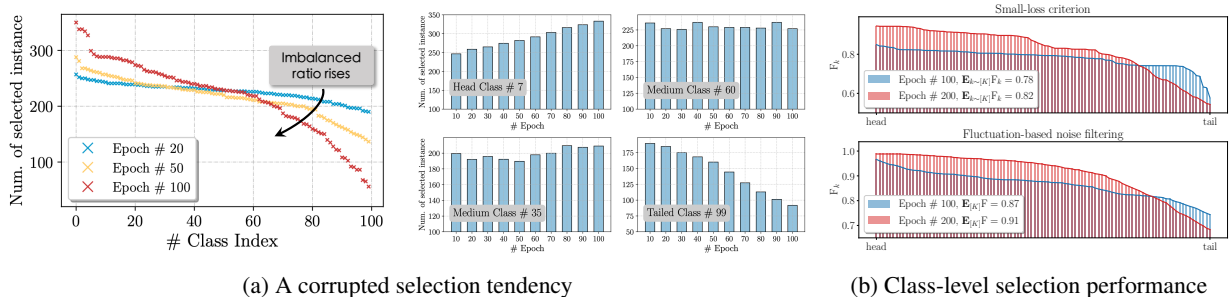


Figure 2: We train ResNet-18 on Sym. 60% CIFAR-100 with small-loss [10] and fluctuation-based noise filtering [11]. (a) Results on small-loss. *Left*: the class distribution of three training stages. *Right*: dynamic numbers of four representative categories. (b) Results on two selection criteria. Visualization of the class-level selection performance F_k in 100- and 200-th epoch. The average F-score among all classes is reported. Although the performance increases, the change is different for varying classes.

[9, 18] introduce the uncertainty of loss to identify the noisy labels. *i.e.*, predictions of noisy instances easily change and thus yield uncertain losses. A recent work [11] points out that hard samples are easily mixed with noisy samples and further discarded by the small-loss criterion. To solve this problem, Wei *et al.* [11] proposed a fluctuation-based sample selection method that considers the samples with inconsistent prediction results as incorrectly labeled data.

Long-tailed classification. Current long-tailed classification methods can be roughly categorized into two strategies, 1) customize the data sampler to modify sampling frequency for different classes (including over-sampling the tail-class samples and under-sampling the head-class samples) [25, 26, 27, 28], and 2) generate class-wise weights of training losses for improving the importance of tailed classes in terms of empirical risk minimization [25, 28, 29, 30, 31, 32]. However, both strategies result in underfitting in the representation of head classes, *i.e.*, the model eventually learns sparse feature representations for head classes [33, 34]. To overcome this issue, some studies [35, 36] leverage the knowledge underlying head classes to promote the learning of tail classes. Cui *et al.* [37] designs a re-balance loss by computing the number of instances from each class and assigning different importance weights. Tang *et al.* [38] leverages causal learning and disentangles feature learning via backdoor adjustment.

Mixture-of-experts. MoE, which belongs to a combination method, has great potential to improve performance in machine learning [39]. Earlier works on MoE mainly focus on dividing the problem space between different experts. Concretely, combining classifiers exhibits promising performance in classification tasks [40, 41], especially for the problem that involves a limited number of patterns, high-dimensional feature sets, and highly overlapped classes [42, 43]. Nowadays, MoE has been applied to several fields, such as long-tailed classification [44, 45] and nature languages processing (NLP) [46, 47].

In this paper, we do not focus on the selection criterion but rather propose a new robust network architecture. Generally, our network can be widely applied to current sample selection methods and further improve their performance.

3 Background

In this section, we first introduce the formal problem setting of learning with noisy labels (LNL) and its learning goal. Then, we conduct experiments to deeply analyze where the bias of sample selection in LNL comes from.

Assume \mathcal{X} is the feature space and $\mathcal{Y} = \{1, 2, \dots, K\}$ is the label space. Suppose the training set is denoted by $D_N = \{(\mathbf{x}_i, y_i)\}_{i \in [N]}$, where $[N] = \{1, 2, \dots, N\}$ is the set of indices. Since the annotator may give wrong labels in practice [48, 49], the learner thus can only observe a label-corrupted set $\tilde{D}_N = \{(\mathbf{x}_i, \tilde{y}_i)\}_{i \in [N]}$.

As a prevailing strategy for LNL, sample selection [9, 11, 12, 50] aims to progressively select a reliable subset $\tilde{D}_M \subseteq \tilde{D}_N$ ($M < N$) and feed \tilde{D}_M to the classifier for training. We introduce $v_i \in \{0, 1\}$ to indicate whether the i -th instance is selected ($v_i = 1$) or not ($v_i = 0$). The performance of selection can be reflected by the F-score F , where $F = \frac{2 \cdot P \cdot R}{P + R}$, P and R denote selection precision and recall, respectively. In this paper, we individually calculate each class's F-score for further analyses, *i.e.*, $F_k = \frac{2 \cdot P_k \cdot R_k}{P_k + R_k}$, $P_k = \frac{\sum_{i \in [N]} \mathbb{1}(v_i = 1, y_i = \tilde{y}_i = k)}{\sum_{i \in [N]} \mathbb{1}(v_i = 1, \tilde{y}_i = k)}$, and $R_k = \frac{\sum_{i \in [N]} \mathbb{1}(v_i = 1, y_i = \tilde{y}_i = k)}{\sum_{i \in [N]} \mathbb{1}(y_i = \tilde{y}_i = k)}$.

By analyzing the selection performance under different training conditions, we have several nontrivial findings.

- *Current selection criteria easily result in an imbalanced selection subset.* As shown in Figure 1, we can observe

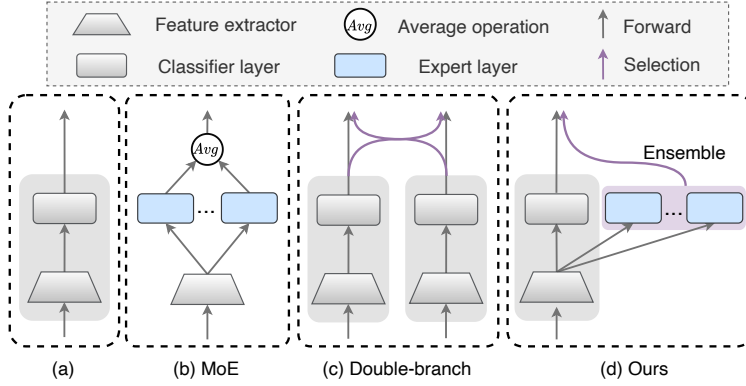


Figure 3: Comparisons of various networks. (a) *Typical classification network*, which consists of a feature extractor and a classifier layer. (b) *Mixture-of-experts (MoE)* [51], a set of experts jointly gives the predicted label for the input. (c) *Double-branch robust structure*, the network is trained on a selected set which is considered as the clean by another network. (d) *Ours*, our framework consists of a classifier layer and a set of expert layers.

that both the two adopted selection strategies incur the imbalanced data distribution under two noisy conditions. The reason is that both the two selection criteria rely on model performance. However, the model has different capacities for different classes. For those classes with indistinguishable characteristics (i.e., tail classes in the figure), the model tends to produce a large loss or inconsistent results and further discards those samples.

- *Sample selection, conducted as self-training, will exacerbate the imbalanced ratio during the training process.* As shown in Figure 2a, the imbalanced ratio of the selected set increases as the training process proceeds, i.e., the number of selected instances increases in head classes and decreases in tail classes (see the right part of Figure 2a). The intuitive reason is that the model’s performance on tail classes hardly improves due to the limited number of available samples for training, which further degrades the effectiveness of selection criteria on these classes.
- *The selection performance is inherently influenced by the imbalanced class distribution.* As shown in Figure 2b, the selection performance of both two selection criteria increases in head classes but decreases in tail classes. The reason is that the selected errors are relatively small for categories with higher F-scores, hence the training of these classes would further improve the model’s accuracy and selection performance. However, for tail classes with lower F-score, the self-training mechanism would further increase the selection error, and thus fail to correctly select instances in the follow-up phase.

In LNL, we are given a label-corrupted training set $\tilde{D}_N = \{(\mathbf{x}_i, \tilde{y}_i)\}_{i \in [N]}$ of N samples. A classifier with learnable parameters f_θ is a function that maps from the input space \mathcal{X} to the label space $f : \mathcal{X} \rightarrow \mathbb{R}^K$. In multi-class classification, we always update the parameter θ by minimizing the following empirical risk:

$$\hat{R}(f) = \frac{1}{N} \sum_{i=1}^N \mathcal{L}(f(\mathbf{x}_i, \theta), \tilde{y}_i), \quad (1)$$

where $\mathcal{L}(\cdot)$ is the given loss function, e.g., Softmax Cross-Entropy (CE) loss. In sample selection strategy, previous works mainly focus on designing high-effectively selection criteria. A universal training objective on the selected clean set can be written as

$$\hat{R}_{\text{clean}}(f) = \frac{1}{N} \sum_{i=1}^N [\text{Criterion}(f, \mathbf{x}_i, \tilde{y}_i) \cdot \mathcal{L}(f(\mathbf{x}_i, \theta), \tilde{y}_i)], \quad \text{where } \text{Criterion}(\cdot) = \begin{cases} 1, & \text{If selected,} \\ 0. & \end{cases} \quad (2)$$

We empirically show that directly optimizing $\hat{R}_{\text{clean}}(f)$ with an existing selection criterion is always biased (in Sec. 3), further resulting in inferior performance. For this, we propose to fulfill debiased learning by handling both the training and data bias. First, to solve the training bias, we design a novel network architecture, called noIse-Tolreant Expert Model (ITEM). Compared with the widely applied double-branch network, our proposal exhibits greater robustness to noisy labels. Second, to solve the data bias, we propose a mixed sampling strategy that can mitigate the side-effect caused by the class-imbalanced set \tilde{D}_{clean} while avoiding sparse representations.

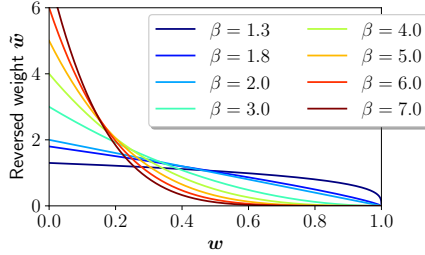


Figure 4: The mapping function $S^\beta(\cdot)$ with varying values of β . Note that $S(\cdot)$ degrades into a transverse line when $\beta = 1$.

3.1 ITEM: noise-Tolerant Expert Model

The training bias of sample selection stems from the way of a self-training manner. Previous works [10, 12] always resort to the double-branch network to confront this problem. Concretely, the network is trained on the clean set that is selected by the other network. Motivated by Mixture-of-experts [41, 51], we propose a robust architecture that integrates multiple experts into the classifier, which independently conducts classifier learning and sample selection in a single network.

Specifically, compared with a normal classification network with a classifier layer f , our network ITEM contains f and a set of expert layers $\{g^1, \dots, g^m\}$ with size m . For robust selection, we propose to conduct existing criteria on expert layers. Therefore, the training objective in our framework can be summarized as

$$\hat{R}_{\text{clean}}(f) = \frac{1}{N} \sum_{i=1}^N [\text{Criterion}(\{g^1, \dots, g^m\}, \mathbf{x}_i, \tilde{y}_i) \cdot \mathcal{L}(f(\mathbf{x}_i, \boldsymbol{\theta}), \tilde{y}_i)].$$

Intuitively, the independent selection phase avoids the classifier layer selecting noisy samples and then updates its parameters on these data, which contributes to mitigating the training bias. We show the comparison of varying networks in Figure 3. Compared with the prevailing double-branch network, which is proved to be noise-robust in previous works [10, 12], our architecture contains two merits, including 1) resource-friendly training, in contrast to the feature extractor’s huge parameters, the last layer’s parameters for classification are significantly fewer. For example, the parameters of the classifier (or the expert) layer are less than 0.01 million, while the total parameters of a single ResNet-18 for CIFAR-10 are roughly 11.1 million. Thus, our network is more friendly to GPU and computer memory. 2) Greater performance, thanks to the property of fewer parameters, our model can integrate more experts, benefiting both selection and test accuracy by ensembling the results.

Remark. *How to update parameters of the expert layer?* All selection criteria depend on the model’s performance, including both small-loss family and fluctuation-based methods. Therefore, leveraging expert layers for selecting without updating parameters easily results in poor selection, even leading to a collapse. To fulfill accurate selection on expert layers, we propose a stochastic updating strategy, which randomly assigns a layer from the set of $\mathbb{F} = \{f, g^1, \dots, g^m\}$ as the classifier layer f^c and the rest are expert layers. Hence, Eq. (3) can be rewritten as

$$\hat{R}_{\text{clean}}(f^c) = \frac{1}{N} \sum_{i=1}^N [\text{Criterion}(\mathbb{F} \setminus f^c, \mathbf{x}_i, \tilde{y}_i) \cdot \mathcal{L}(f^c(\mathbf{x}_i, \boldsymbol{\theta}), \tilde{y}_i)]. \quad (3)$$

Since sufficient training processes, we consider that each layer in ITEM contains remarkable performance on selection and prediction.

3.2 Mixed Sampling

To overcome the data bias, we propose a Mixed Sampling strategy to simultaneously learn from head and tail classes in each training iteration. Specifically, supposing a clean set \tilde{D}_{clean} is selected from the \tilde{D}_N , where $\tilde{D}_{\text{clean}} \subseteq \tilde{D}_N$. By calculating the number of instances from each class in \tilde{D}_{clean} and conducting L1 normalization, a vector of class weights $\mathbf{v} = [w_1, \dots, w_K]$ can be obtained. The weight of class k is written as

$$\mathbf{w}_k = \text{Normalize}(S_k) = u_k / \sum_{i=1}^K u_i, \quad (4)$$

where u_i denotes the quantity of i -th class in \tilde{D}_{clean} .

Algorithm 1 ITEM

Input: Noisy training set \tilde{D}_N , training epoch T , warmup iterations T_w , a selection criterion $\text{Criterion}(\cdot)$, a classifier network with m experts, the mapping function $\mathcal{S}^\beta(\cdot)$ with a hyper-parameter β .

- 1: **Initialize** our network with one classifier layer and m expert layers $\mathbb{F} = \{f, g^1, \dots, g^m\}$.
 - 2: **for** $t = 1, \dots, T_w$ **do**
 - 3: Randomly sample f^c from \mathbb{F} , and WarmUp f^c on D_N .
 - 4: **end for**
 - 5: **for** $t = 1, \dots, T$ **do**
 - 6: Select the clean set \tilde{D}_{clean} from D_N based on $\text{Criterion}(\mathbb{F})$.
 - 7: Calculate weighted vector $\mathbf{v} = [\mathbf{w}_1, \dots, \mathbf{w}_K]$ on \tilde{D}_{clean} .
 - 8: Calculate reversed weighted vector $\tilde{\mathbf{v}} = [\tilde{\mathbf{w}}_1, \dots, \tilde{\mathbf{w}}_K]$ with Eq. (5).
 - 9: **while** $i = 1, \dots$, iterations **do**
 - 10: Randomly sample a mini batch $B_{\mathbf{v}} = \{(\mathbf{x}_i, \tilde{y}_i)\}_{i=1}^b$ from \tilde{D}_{clean} according to \mathbf{v} .
 - 11: Randomly sample a mini-batch $B_{\tilde{\mathbf{v}}} = \{(\mathbf{x}'_i, \tilde{y}'_i)\}_{i=1}^b$ from \tilde{D}_{clean} according to $\tilde{\mathbf{v}}$.
 - 12: Randomly sample f^c from \mathbb{F} .
 - 13: Update the network parameters by minimizing $\frac{1}{b} \sum_{i=1}^b \mathcal{L}(f^c(\text{MixUp}(\mathbf{x}_i, \mathbf{x}'_i)), \text{MixUp}(\tilde{y}_i, \tilde{y}'_i))$.
 - 14: **end while**
 - 15: **end for**
-

Based on the weight vector \mathbf{v} , we further propose a reversed weight vector that assigns a larger weight to tailed classes when sampling. Concretely, we construct a mapping function based on the probability density function (PDF) of a Beta distribution. Normally, the Beta distribution’s PDF is controlled by two parameters α, β . To satisfy both 1) the input interval of \mathbf{w}_k belongs to $\{0, 1\}$ and 2) the function contains the monotonically decreasing property, we thus fix $\alpha = 1$ and adjust β to achieve different slopes. Given a weight \mathbf{w} , the reversed weight $\tilde{\mathbf{w}}$ can be obtained by our mapping function, which is written as

$$\tilde{\mathbf{w}} = \mathcal{S}^\beta(\mathbf{w}) = \frac{1}{\text{B}(1, \beta)} (1 - \mathbf{w})^{\beta-1}, \quad (5)$$

where β is a hyperparameter and $\text{B}(\cdot)$ denotes a beta function written as $\text{B}(1, \beta) = \int_0^1 (1-t)^{\beta-1} dt$. The mapping function $\mathcal{S}^\beta(\cdot)$ with varying values of β is shown in Figure 4. We observe that given an input with a larger weight, the output value becomes smaller. Therefore, we can gain a reversed weight vector $\tilde{\mathbf{v}} = [\tilde{\mathbf{w}}_1, \dots, \tilde{\mathbf{w}}_K]$ that gives a smaller weight to the class with a large number. By weighted sampling with $\tilde{\mathbf{v}}$, a training mini-batch $B_{\tilde{\mathbf{v}}}$ mainly contains tail classes can be obtained.

Training on the tail-focused training batch directly would result in the sparse representation of head classes [52]. To avoid this problem, we separately conduct two times weighted sampling (according to the weighted and reversed weighted vector $\mathbf{v}, \tilde{\mathbf{v}}$) in data loader phase. Then, we have two training mini-batches $B_{\mathbf{v}}$ and $B_{\tilde{\mathbf{v}}}$, which focus on head and tail classes, respectively. By leveraging MixUp strategy [22], the model can learn a more representative feature extractor on the mixed data $\text{MixUp}(B_{\mathbf{v}}, B_{\tilde{\mathbf{v}}})$.

3.3 Practical Training

Despite the training objective of selection-based methods being summarized as a joint framework (in Eq. (3)), the training procedure is practically decoupled into two stages that are iteratively proceeding, 1) select clean samples via the preset criterion and 2) train the network on the selected set. Our training manner also obeys this framework.

Specifically, supposing a selection criterion $\text{Criterion}(\cdot)$ such as small-loss [10] or fluctuation-based noise filtering [11] and a network with m size expert layer. In each training epoch, the clean set \tilde{D}_{clean} is selected. To calculate the number of each class in \tilde{D}_{clean} , we have a weighted vector \mathbf{v} . Then, the reversed vector $\tilde{\mathbf{v}}$ is obtained via the mapping function (in Eq. (5)). In each training iteration, we respectively sample a head-focused batch $B_{\mathbf{v}} = \{(\mathbf{x}_i, \tilde{y}_i)\}_{i=1}^b$ and a tail-focused batch $B_{\tilde{\mathbf{v}}} = \{(\mathbf{x}'_i, \tilde{y}'_i)\}_{i=1}^b$ from \tilde{D}_{clean} according to $\tilde{\mathbf{v}}$, where b denote the size of the mini-batch. By randomly selecting a layer from \mathbb{F} as the classifier layer f^c , the parameter’s update can be achieved by minimizing the following training loss

$$L^{\text{train}} = \frac{1}{b} \sum_{i=1}^b \mathcal{L}(f^c(\text{MixUp}(\mathbf{x}_i, \mathbf{x}'_i)), \text{MixUp}(\tilde{y}_i, \tilde{y}'_i)), \quad (6)$$

Table 1: Test accuracy (mean \pm std) of methods using ResNet-18/34 on CIFAR-10/100. Note that †, ‡ and † denote three selection criteria, *i.e.*, small-loss detection with loss threshold [10], small-loss detection with Gaussian Mixture Model [12], and fluctuation-based noise filtering [11]. **Bold** values denote the best the second best performance.

	Methods	Sym. 20%	Sym. 40%	Inst. 20%	Inst. 40%	Avg.
CIFAR-10	Cross-Entropy [53]	85.00 \pm 0.43%	79.59 \pm 1.31%	85.92 \pm 1.09%	79.91 \pm 1.41%	82.61
	MentorNet [54]	80.49 \pm 0.11%	77.48 \pm 3.45%	79.12 \pm 0.42%	70.27 \pm 1.52%	76.84
	JoCoR [8]	88.69 \pm 0.19%	85.44 \pm 0.29%	87.31 \pm 0.27%	82.49 \pm 0.57%	85.98
	Joint Optim [55]	89.70 \pm 0.36%	87.79 \pm 0.20%	89.69 \pm 0.42%	82.62 \pm 0.57%	87.45
	CDR [23]	89.68 \pm 0.38%	86.13 \pm 0.44%	90.24 \pm 0.39%	83.07 \pm 1.33%	87.28
	Me-Momentum [16]	91.44 \pm 0.33%	88.39 \pm 0.34%	90.86 \pm 0.21%	86.66 \pm 0.91%	89.34
	PES [56]	92.38 \pm 0.41%	87.45 \pm 0.34%	92.69 \pm 0.42%	89.73 \pm 0.51%	90.56
	Late Stopping [19]	91.06 \pm 0.22%	88.92 \pm 0.38%	91.08 \pm 0.23%	87.41 \pm 0.38%	89.62
	† Co-teaching [10]	87.16 \pm 0.52%	83.59 \pm 0.28%	86.54 \pm 0.11%	80.98 \pm 0.39%	84.56
	† ITEM (Ours)	93.79 \pm 0.14%	90.83 \pm 0.19%	93.52 \pm 0.14%	91.09 \pm 0.18%	92.31
	‡ ITEM (Ours)	95.01 \pm 0.21%	93.10 \pm 0.20%	95.18 \pm 0.19%	93.65 \pm 0.12%	94.24
	† SFT [11]	92.57 \pm 0.32%	89.54 \pm 0.27%	91.41 \pm 0.32%	89.97 \pm 0.49%	90.87
‡ ITEM (Ours)	95.26 \pm 0.23%	92.81 \pm 0.20%	95.80 \pm 0.18%	93.13 \pm 0.29%	94.25	
CIFAR-100	Cross-Entropy [53]	57.59 \pm 2.55%	45.74 \pm 2.61%	59.85 \pm 1.56%	43.74 \pm 1.54%	51.73
	MentorNet [54]	52.11 \pm 0.10%	35.12 \pm 1.13%	51.73 \pm 0.17%	40.90 \pm 0.45%	44.96
	JoCoR [8]	64.17 \pm 0.19%	55.97 \pm 0.46%	61.98 \pm 0.39%	50.59 \pm 0.71%	58.17
	Joint Optim [55]	64.55 \pm 0.38%	57.97 \pm 0.67%	65.15 \pm 0.31%	55.57 \pm 0.41%	60.81
	CDR [23]	66.52 \pm 0.24%	60.18 \pm 0.22%	67.06 \pm 0.50%	56.86 \pm 0.62%	62.65
	Me-Momentum [16]	68.03 \pm 0.53%	63.48 \pm 0.72%	68.11 \pm 0.57%	58.38 \pm 1.28%	64.50
	PES [56]	68.89 \pm 0.41%	64.90 \pm 0.57%	70.49 \pm 0.72%	65.68 \pm 0.44%	67.49
	Late Stopping [19]	68.67 \pm 0.67%	64.10 \pm 0.40%	68.59 \pm 0.70%	59.28 \pm 0.46%	65.16
	† Co-teaching [10]	59.28 \pm 0.47%	51.60 \pm 0.49%	57.24 \pm 0.69%	45.69 \pm 0.99%	53.45
	† ITEM (Ours)	72.42 \pm 0.17%	71.96 \pm 0.24%	73.61 \pm 0.16%	69.90 \pm 0.30%	71.97
	‡ ITEM (Ours)	78.20 \pm 0.09%	75.27 \pm 0.20%	77.91 \pm 0.14%	70.69 \pm 0.31%	75.51
	† SFT [11]	71.98 \pm 0.26%	69.72 \pm 0.31%	71.83 \pm 0.42%	69.91 \pm 0.54%	70.86
‡ ITEM (Ours)	77.19 \pm 0.13%	74.90 \pm 0.24%	76.91 \pm 0.23%	71.44 \pm 0.29%	75.11	

where $\text{MixUp}(\cdot)$ is represented as $\text{MixUp}(a, b) = \gamma \cdot a + (1 - \gamma) \cdot b$ and γ is a trade-off coefficient randomly sampled from a beta distribution $\text{beta}(\alpha, \alpha)$. The algorithm flowchart of ITEM is shown in Algorithm 1.

4 Experiments

Datasets. We assess the performance of *ITEM* on two noise-synthetic datasets CIFAR-10 and CIFAR-100 [48], and two real-world noisy datasets CIFAR-10N [57] and Clothing-1M [58]. To manually generate the noise, we follow the work [8] and construct *symmetric* and *instance-dependent* label noise on CIFAR-10 and CIFAR-10. Specifically, given a noise ratio ρ , symmetric label noise randomly translates the true label to a wrong label with probability ρ , while instance-dependent label noise assumes a corresponding relationship exists in input features [59]. In experiments, we set the $\rho \in \{20\%, 40\%\}$. For testing real-world performance, we employ CIFAR-10N, a human-annotated dataset with varying noise conditions, including *worst* and *random 1&2&3*. Besides, Clothing-1M [58], a large-scale dataset that is collected from the website and contains one million training data with 14 categories, is also utilized.

Compared methods. On CIFAR-10 & 100, we compare ITEM with prevailing methods that can be roughly divided into three parts, including 1) sample selection methods (small-loss), MentorNet [54], JoCoR [8], and Me-Momentum [16], 2) sample selection methods (fluctuation), SFT [11] and Late Stopping [19], 3) others, Cross-Entropy [53], Joint Optim [55], and PES [56]. Note that all reported results in this paper are collected from SFT and Late Stopping. On the real-world dataset CIFAR-10N, we compare ITEM with Co-teaching+ [14], Peer Loss [60], CAL [61], DivideMix [12], ELR+ [15], and CORES* [59]. The results are collected from the literature [57].

Experimental setup. We keep the convention from [11, 19] and adopt ResNet-18 and ResNet-34 for CIFAR-10 and CIFAR-100, respectively. For all noisy conditions on CIFAR-10 & 100, we leverage an SGD optimizer with the momentum 0.9 and the weight-decay 1e-3 to train our network. The total training epoch is set as 200. The initial learning rate is 0.02 and decayed with the factor 10 at the 100-th and 150-th epoch. For real-world noise, ResNet-34 and a pre-trained ResNet-50 are used for Clothing-1M and CIFAR-10N, respectively. More details can be found in the

Table 2: Test accuracy (%) of prevailing methods using ResNet-34 on CIFAR-10N. Note that ✓ and ✗ indicate whether a *semi-supervised framework* is used or not. More results about CIFAR-100N are shown in Appendix B.1.

Methods		CIFAR-10N			
		<i>Worst</i>	<i>R. 1</i>	<i>R. 2</i>	<i>R. 3</i>
CE	✗	77.69	85.02	86.46	85.16
Co-teaching+	✗	83.26	89.70	89.47	89.54
Peer Loss	✗	82.00	89.06	88.76	88.57
CAL	✗	85.36	90.93	90.75	90.74
Late Stopping	✗	85.27	-	-	-
‡ ITEM	✗	91.15	95.12	95.03	95.17
DivideMix	✓	92.56	95.16	95.23	95.21
ELR+	✓	91.09	94.43	94.20	94.34
CORES*	✓	91.66	94.45	94.88	94.74
‡ ITEM*	✓	93.14	96.08	96.54	96.71

Table 3: Test accuracy (%) of prevailing methods using the pretrained ResNet-50 on Clothing-1M.

Methods	Test acc. (%)	Methods	Test acc. (%)
CE	64.54	Co-teaching	69.21
Forward	69.84	SFT+	75.08
JoCoR	70.30	DMI	72.46
Joint Optim	72.23	PES (semi)	74.85
DivideMix	74.76	ELR+	74.81
‡ ITEM	74.69	‡ ITEM*	75.02

Table in Appendix C.

Hyperparameter setup. Our framework contains two main hyperparameters, *i.e.*, the number of expert m in the network architecture, and the slope parameter β in the mapping function. We keep $\beta = 2$ for all experiments and set $m = 2, 4$ for CIFAR and Clothing-1M, respectively.

4.1 Comparison Results

Results on CIFAR-10 and CIFAR-100. Since our framework is not restricted by different selection criteria, we test our proposal on three types of selection criterion, including small-loss with loss threshold [10], small-loss with Gaussian Mixture Model [12] and fluctuation-based noise filtering [11]. Each trial is repeated five times with different seeds. Mean values with standard deviation are recorded.

Experimental results are shown in Table 1. On both CIFAR-10 and CIFAR-100, our method ITEM consistently achieves state-of-the-art performance on all noisy settings. Compared with other section-based methods such as Co-teaching and SFT, ITEM obtains obvious performance improvements while adopting their selection criteria. To be specific, †ITEM averagely improves the test accuracy of Co-teaching by 9.68% on CIFAR-10 and 22.06% on CIFAR-100. Compared with SFT, a representative method in fluctuation-based selection, ITEM also achieves remarkable improvements. Meanwhile, our model exhibits greater generalization performance on more challenging dataset, *e.g.*, the improvement on CIFAR-100 *v.s.* CIFAR-10.

Results on CIFAR-10N. We evaluate the effectiveness of ITEM on a human-annotated noisy dataset CIFAR-10N which contains four noisy conditions, *i.e.*, *Worst* and *Random 1&2&3* [57]. Besides, following previous selection-based approaches [12], we discard labels of unreliable samples and train the model with them by semi-supervised learning (SSL) for greater generalization, which is represented as ITEM*. Appendix A shows the detailed algorithm flowchart for ITEM*.

The results can be found in Table 2. First, our method achieves remarkable performance on both two settings (*w/* or *w/o* SSL). When training without SSL, ITEM outperforms previous methods by a large margin. Compared with Late Stopping, a newly proposed method, ITEM achieves 5.88% improvements on *worst*-labels. When training with SSL, ITEM is also superior to the previous SOTA method DivideMix. It is worth noting that even training without SSL, ITEM surprisingly gains greater performance than those methods that leverage SSL approaches.

Table 4: Test accuracy (%) of prevailing methods using the ResNet-32 on imbalanced noisy CIFAR-10/100. Note that ξ and ρ denote the *imbalanced ratio* and the *noise ratio*, respectively. The best and the second best performance are highlighted with **bold** and underline, respectively.

		ξ	10				
		ρ	10%	20%	30%	40%	50%
CIFAR-10	Co-teaching		80.30	78.54	68.71	57.10	46.77
	Sel-CL+		86.47	85.11	84.41	80.35	77.27
	RCAL		88.09	86.46	<u>84.58</u>	<u>83.43</u>	<u>80.80</u>
	Ours		<u>87.32</u>	<u>86.31</u>	84.91	84.72	81.04
CIFAR-100	Co-teaching		45.61	41.33	36.14	32.08	25.33
	Sel-CL+		55.68	53.52	50.92	47.57	44.86
	RCAL		57.50	<u>54.85</u>	<u>51.66</u>	48.91	44.36
	Ours		<u>56.10</u>	55.93	53.07	<u>48.29</u>	45.17

Table 5: Ablation study of each component in \ddagger ITEM with varying noise conditions.

Methods	CIFAR-10		CIFAR-100		CIFAR-10N
	Sym 40%	Inst. 40%	Sym 40%	Inst. 40%	Worst
w/o robust multi-expert network (training on normal ResNet)	90.75	91.44	73.01	70.04	89.72
w/o mixed sampling (training on a random sampled batch)	88.77	89.91	71.09	68.54	87.66
w/o mixup (directly training on Bv and $B\bar{v}$)	90.19	90.35	72.50	69.11	89.10
Ours	92.81	93.13	74.90	71.44	91.15

Results on Clothing-1M. Going beyond the small-scale benchmark such as CIFAR-10 & 100, we also test the performance of ITEM and ITEM* on a large-scale dataset Clothing-1M, which contains roughly 38.49% noisy labels. The results are shown in Table 3. We can observe that both ITEM and ITEM* outperform existing methods by a meaningful margin. For example, ITEM* achieves 0.17% improvements compared with the second-best method PES. The result verifies that our method is effective for enhancing model generalization in large-scale real-world scenarios.

4.2 More Analyses

Versatility. Recently, some studies [62, 63] studied a more challenging noise learning task, i.e., learning with noisy labels on imbalanced datasets, which is a more realistic scenario. Thanks to the class-aware data sampling strategy in ITEM, our method can also tackle this task. Following the imbalanced noise setting and experimental setup of RCAL [62], we verify the performance of \ddagger ITEM on comprehensive conditions. Experimental details can be found in Appendix C.1 and results are shown in Table 4. On CIFAR-10, ITEM exhibits greater generalization under a high noise ratio. For example, ITEM outperforms RCAL by 1.29% and 0.24% under 40% and 50% noise ratio, respectively. On CIFAR-100, ITEM also achieves competitive performance, i.e., the best or the second-best performance. Therefore, ITEM can be applied to more general scenarios.

Ablation study. Our framework mainly contains two modules, the robust network architecture and the mixed data sampling strategy. We conduct ablation studies on CIFAR benchmarks to evaluate the effectiveness of each component (shown in Table 5). First, compared with typical ResNet architecture, our expert-based network indeed makes an obvious contribution to mitigating the noise. The average improvement among five noisy settings roughly reaches 2%. Second, the mixed sampling strategy also promotes the performance of our network. Note that compared with training on randomly sampled batches, training on two weighted sampled batches gains greater generalization. Thus, each module in our learning framework is effective.

Hyperparameter selection. There are two main hyperparameters m and β in our framework. We conduct ablation studies to select optimal values for experiments, where $m \in \{2, 3, 4, 5, 6, 7, 8\}$ and $\beta \in \{1.3, 1.8, 2, 3, 5, 10\}$. The result is shown in Figure 5. For the number of expert layers, we can see that the best test accuracy increases with a larger value of m . When $m = 4$, the performance reaches the peak and slightly fluctuates as m increases. Meanwhile, the gap between the peak value and the least value is around 0.6% on CIFAR-10 and 0.9% on CIFAR-100, respectively. For the slope parameter in the mapping function, we observe that the performance of our framework is not sensitive to varying values of β . Therefore, we select $m = 4$ and $\beta = 3$ for all experiments.

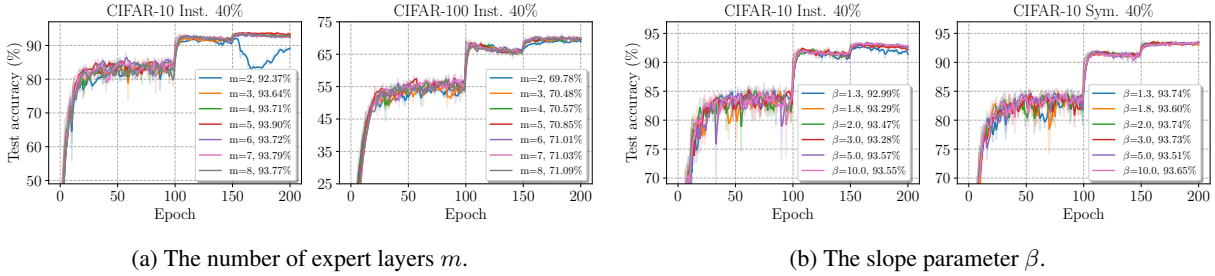


Figure 5: Sensitivity analyses for hyperparameters selection.

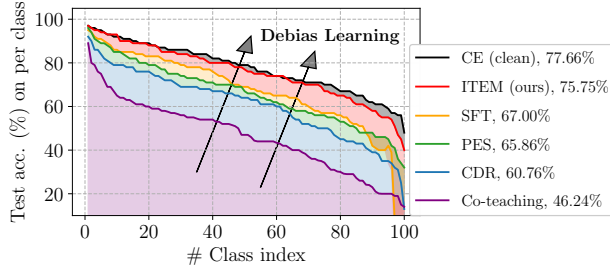


Figure 6: Comparisons of class-level prediction results on CIFAR-100 with 40% symmetric noise. Note that “CE (clean)” denotes training the model on the completely clean set (50k samples).

Class-balanced learning. We visualize the test accuracy in each class to demonstrate that ITEM achieves relatively balanced performance on varying categories while fulfilling greater generalization. We plot comparison results in Figure 6. First, compared with *CE (clean)*, which is trained on 50k clean samples, ITEM achieves almost unbiased prediction results. Second, compared with existing methods, ITEM takes tail classes better into account since two weighted samplers. Therefore, ITEM obtains greater performance in these categories. The result demonstrates our proposal has considerable potential in fulfilling class-balanced learning while tackling label noise.

5 Conclusion

In this paper, we disclosed the data bias, an implicit bias underlying the sample selection strategy. To solve the training and data bias simultaneously, we proposed ITEM, which integrates a noise-robust multi-experts network and a mixed sampling strategy. First, our structure integrates the classifier with multiple experts and leverages expert layers to conduct selection independently. Compared with the prevailing double-branch network, it exhibits great potential in mitigating the training bias, i.e., the accumulated error. Second, our mixed sampling strategy yields class-aware weights and further conducts weighted sampling. By using the mixup of two weighted mini-batches, we mitigate the issue of sparse representation. The effectiveness of ITEM in real applications is verified on diverse noise types and both synthetic and real-world datasets.

References

- [1] H. Shen, Z.-Q. Zhao, Y. Zhang, and Z. Zhang, “Mutual information-driven triple interaction network for efficient image dehazing,” in *ACM MM*, pp. 7–16, 2023.
- [2] H. Shen, Z.-Q. Zhao, and W. Zhang, “Adaptive dynamic filtering network for image denoising,” in *AAAI*, vol. 37, pp. 2227–2235, 2023.
- [3] A. Blum, A. Kalai, and H. Wasserman, “Noise-tolerant learning, the parity problem, and the statistical query model,” *Journal of the ACM (JACM)*, vol. 50, no. 4, pp. 506–519, 2003.
- [4] Y. Yan, R. Rosales, G. Fung, R. Subramanian, and J. Dy, “Learning from multiple annotators with varying expertise,” *Machine learning*, vol. 95, pp. 291–327, 2014.

- [5] Q. Wei, L. Feng, H. Sun, R. Wang, C. Guo, and Y. Yin, “Fine-grained classification with noisy labels,” in *CVPR*, pp. 11651–11660, 2023.
- [6] C. Zhang, S. Bengio, M. Hardt, B. Recht, and O. Vinyals, “Understanding deep learning requires rethinking generalization,” in *ICLR*, 2017.
- [7] H. Sun, C. Guo, Q. Wei, Z. Han, and Y. Yin, “Learning to rectify for robust learning with noisy labels,” *Pattern Recognition*, vol. 124, p. 108467, 2022.
- [8] H. Wei, L. Feng, X. Chen, and B. An, “Combating noisy labels by agreement: A joint training method with co-regularization,” in *CVPR*, pp. 13726–13735, 2020.
- [9] X. Xia, T. Liu, B. Han, M. Gong, J. Yu, G. Niu, and M. Sugiyama, “Sample selection with uncertainty of losses for learning with noisy labels,” in *ICLR*, 2022.
- [10] B. Han, Q. Yao, X. Yu, G. Niu, M. Xu, W. Hu, I. Tsang, and M. Sugiyama, “Co-teaching: Robust training of deep neural networks with extremely noisy labels,” in *NeurIPS*, vol. 31, 2018.
- [11] Q. Wei, H. Sun, X. Lu, and Y. Yin, “Self-filtering: A noise-aware sample selection for label noise with confidence penalization,” in *ECCV*, pp. 516–532, Springer, 2022.
- [12] J. Li, R. Socher, and S. C. Hoi, “Dividemix: Learning with noisy labels as semi-supervised learning,” in *ICLR*, 2020.
- [13] Y. Xu, P. Cao, Y. Kong, and Y. Wang, “L_dmi: A novel information-theoretic loss function for training deep nets robust to label noise,” in *NeurIPS*, vol. 32, 2019.
- [14] X. Yu, B. Han, J. Yao, G. Niu, I. Tsang, and M. Sugiyama, “How does disagreement help generalization against label corruption?,” in *ICML*, pp. 7164–7173, PMLR, 2019.
- [15] S. Liu, J. Niles-Weed, N. Razavian, and C. Fernandez-Granda, “Early-learning regularization prevents memorization of noisy labels,” in *NeurIPS*, vol. 33, pp. 20331–20342, 2020.
- [16] Y. Bai and T. Liu, “Me-momentum: Extracting hard confident examples from noisily labeled data,” in *ICCV*, pp. 9312–9321, 2021.
- [17] D. Arpit, S. Jastrzebski, N. Ballas, D. Krueger, E. Bengio, M. S. Kanwal, T. Maharaj, A. Fischer, A. Courville, Y. Bengio, *et al.*, “A closer look at memorization in deep networks,” in *ICML*, pp. 233–242, PMLR, 2017.
- [18] T. Zhou, S. Wang, and J. Bilmes, “Robust curriculum learning: From clean label detection to noisy label self-correction,” in *ICLR*, 2020.
- [19] S. Yuan, L. Feng, and T. Liu, “Late stopping: Avoiding confidently learning from mislabeled examples,” in *ICCV*, pp. 16079–16088, 2023.
- [20] X. Dong, Z. Yu, W. Cao, Y. Shi, and Q. Ma, “A survey on ensemble learning,” *Frontiers of Computer Science*, vol. 14, pp. 241–258, 2020.
- [21] D. Barber and C. Bishop, “Ensemble learning for multi-layer networks,” *NeurIPS*, vol. 10, 1997.
- [22] H. Zhang, M. Cisse, Y. N. Dauphin, and D. Lopez-Paz, “mixup: Beyond empirical risk minimization,” *arXiv preprint arXiv:1710.09412*, 2017.
- [23] X. Xia, T. Liu, B. Han, C. Gong, N. Wang, Z. Ge, and Y. Chang, “Robust early-learning: Hindering the memorization of noisy labels,” in *ICLR*, 2020.
- [24] C. Tan, J. Xia, L. Wu, and S. Z. Li, “Co-learning: Learning from noisy labels with self-supervision,” in *ACM MM*, pp. 1405–1413, 2021.
- [25] M. Buda, A. Maki, and M. A. Mazurowski, “A systematic study of the class imbalance problem in convolutional neural networks,” *Neural networks*, vol. 106, pp. 249–259, 2018.

- [26] J. Byrd and Z. Lipton, “What is the effect of importance weighting in deep learning?,” in *ICML*, pp. 872–881, PMLR, 2019.
- [27] H. He and E. A. Garcia, “Learning from imbalanced data,” *IEEE Transactions on knowledge and data engineering*, vol. 21, no. 9, pp. 1263–1284, 2009.
- [28] N. Japkowicz and S. Stephen, “The class imbalance problem: A systematic study,” *Intelligent data analysis*, vol. 6, no. 5, pp. 429–449, 2002.
- [29] R. Akbani, S. Kwek, and N. Japkowicz, “Applying support vector machines to imbalanced datasets,” in *ECML*, pp. 39–50, Springer, 2004.
- [30] X.-Y. Liu and Z.-H. Zhou, “The influence of class imbalance on cost-sensitive learning: An empirical study,” in *ICDM*, pp. 970–974, IEEE, 2006.
- [31] D. Margineantu, “When does imbalanced data require more than cost-sensitive learning,” in *AAAI Workshop*, pp. 47–50, 2000.
- [32] Z.-H. Zhou and X.-Y. Liu, “Training cost-sensitive neural networks with methods addressing the class imbalance problem,” *IEEE TKDE*, vol. 18, no. 1, pp. 63–77, 2005.
- [33] K. Cao, C. Wei, A. Gaidon, N. Arechiga, and T. Ma, “Learning imbalanced datasets with label-distribution-aware margin loss,” in *NeurIPS*, vol. 32, 2019.
- [34] Y. Yang and Z. Xu, “Rethinking the value of labels for improving class-imbalanced learning,” in *NeurIPS*, vol. 33, pp. 19290–19301, 2020.
- [35] Z. Liu, Z. Miao, X. Zhan, J. Wang, B. Gong, and S. X. Yu, “Large-scale long-tailed recognition in an open world,” in *CVPR*, pp. 2537–2546, 2019.
- [36] Y.-X. Wang, D. Ramanan, and M. Hebert, “Learning to model the tail,” in *NeurIPS*, vol. 30, 2017.
- [37] Y. Cui, M. Jia, T.-Y. Lin, Y. Song, and S. Belongie, “Class-balanced loss based on effective number of samples,” in *CVPR*, pp. 9268–9277, 2019.
- [38] K. Tang, J. Huang, and H. Zhang, “Long-tailed classification by keeping the good and removing the bad momentum causal effect,” in *NeurIPS*, vol. 33, pp. 1513–1524, 2020.
- [39] S. B. Kotsiantis, I. D. Zaharakis, and P. E. Pintelas, “Machine learning: a review of classification and combining techniques,” *Artificial Intelligence Review*, vol. 26, pp. 159–190, 2006.
- [40] A. C. Lorena, A. C. De Carvalho, and J. M. Gama, “A review on the combination of binary classifiers in multiclass problems,” *Artificial Intelligence Review*, vol. 30, pp. 19–37, 2008.
- [41] L. Rokach, “Ensemble-based classifiers,” *Artificial intelligence review*, vol. 33, pp. 1–39, 2010.
- [42] T. P. Tran, T. T. S. Nguyen, P. Tsai, and X. Kong, “Bspnn: boosted subspace probabilistic neural network for email security,” *Artificial Intelligence Review*, vol. 35, no. 4, pp. 369–382, 2011.
- [43] S. B. Kotsiantis, “An incremental ensemble of classifiers,” *Artificial Intelligence Review*, vol. 36, pp. 249–266, 2011.
- [44] X. Wang, L. Lian, Z. Miao, Z. Liu, and S. X. Yu, “Long-tailed recognition by routing diverse distribution-aware experts,” in *ICLR*, 2020.
- [45] L. Xiang, G. Ding, and J. Han, “Learning from multiple experts: Self-paced knowledge distillation for long-tailed classification,” in *ECCV*, pp. 247–263, Springer, 2020.
- [46] S. Zuo, X. Liu, J. Jiao, Y. J. Kim, H. Hassan, R. Zhang, T. Zhao, and J. Gao, “Taming sparsely activated transformer with stochastic experts,” in *ICLR*, 2021.

- [47] Y. Zhou, T. Lei, H. Liu, N. Du, Y. Huang, V. Zhao, A. M. Dai, Q. V. Le, J. Laudon, *et al.*, “Mixture-of-experts with expert choice routing,” in *NeurIPS*, vol. 35, pp. 7103–7114, 2022.
- [48] A. Krizhevsky, I. Sutskever, and G. E. Hinton, “Imagenet classification with deep convolutional neural networks,” in *NeurIPS*, vol. 25, 2012.
- [49] V. Agarwal, T. Podchiyska, J. M. Banda, V. Goel, T. I. Leung, E. P. Minty, T. E. Sweeney, E. Gyang, and N. H. Shah, “Learning statistical models of phenotypes using noisy labeled training data,” *Journal of the American Medical Informatics Association*, vol. 23, no. 6, pp. 1166–1173, 2016.
- [50] Y. Li, H. Han, S. Shan, and X. Chen, “Disc: Learning from noisy labels via dynamic instance-specific selection and correction,” in *CVPR*, pp. 24070–24079, 2023.
- [51] S. Masoudnia and R. Ebrahimpour, “Mixture of experts: a literature survey,” *Artificial Intelligence Review*, vol. 42, pp. 275–293, 2014.
- [52] B. Zhou, Q. Cui, X.-S. Wei, and Z.-M. Chen, “Bbn: Bilateral-branch network with cumulative learning for long-tailed visual recognition,” in *CVPR*, pp. 9719–9728, 2020.
- [53] R. Rubinstein, “The cross-entropy method for combinatorial and continuous optimization,” *Methodology and computing in applied probability*, vol. 1, pp. 127–190, 1999.
- [54] L. Jiang, Z. Zhou, T. Leung, L.-J. Li, and L. Fei-Fei, “Mentornet: Learning data-driven curriculum for very deep neural networks on corrupted labels,” in *ICML*, pp. 2304–2313, PMLR, 2018.
- [55] D. Tanaka, D. Ikami, T. Yamasaki, and K. Aizawa, “Joint optimization framework for learning with noisy labels,” in *CVPR*, pp. 5552–5560, 2018.
- [56] Y. Bai, E. Yang, B. Han, Y. Yang, J. Li, Y. Mao, G. Niu, and T. Liu, “Understanding and improving early stopping for learning with noisy labels,” in *NeurIPS*, vol. 34, pp. 24392–24403, 2021.
- [57] J. Wei, Z. Zhu, H. Cheng, T. Liu, G. Niu, and Y. Liu, “Learning with noisy labels revisited: A study using real-world human annotations,” *arXiv preprint arXiv:2110.12088*, 2021.
- [58] T. Xiao, T. Xia, Y. Yang, C. Huang, and X. Wang, “Learning from massive noisy labeled data for image classification,” in *CVPR*, pp. 2691–2699, 2015.
- [59] H. Cheng, Z. Zhu, X. Li, Y. Gong, X. Sun, and Y. Liu, “Learning with instance-dependent label noise: A sample sieve approach,” *ICLR*, 2021.
- [60] Y. Liu and H. Guo, “Peer loss functions: Learning from noisy labels without knowing noise rates,” in *ICML*, pp. 6226–6236, PMLR, 2020.
- [61] Z. Zhu, T. Liu, and Y. Liu, “A second-order approach to learning with instance-dependent label noise,” in *CVPR*, pp. 10113–10123, 2021.
- [62] M. Zhang, X. Zhao, J. Yao, C. Yuan, and W. Huang, “When noisy labels meet long tail dilemmas: A representation calibration method,” in *ICCV*, pp. 15890–15900, 2023.
- [63] S. Jiang, J. Li, Y. Wang, B. Huang, Z. Zhang, and T. Xu, “Delving into sample loss curve to embrace noisy and imbalanced data,” in *AAAI*, vol. 36, pp. 7024–7032, 2022.
- [64] K. Sohn, D. Berthelot, N. Carlini, Z. Zhang, H. Zhang, C. A. Raffel, E. D. Cubuk, A. Kurakin, and C.-L. Li, “Fixmatch: Simplifying semi-supervised learning with consistency and confidence,” *NeurIPS*, vol. 33, pp. 596–608, 2020.
- [65] A. Khosla, N. Jayadevaprakash, B. Yao, and L. Fei-Fei, “Novel dataset for fine-grained image categorization,” in *Workshop on CVPR*, 2011.
- [66] P. Welinder, S. Branson, T. Mita, C. Wah, F. Schroff, S. Belongie, and P. Perona, “Caltech-ucsd birds 200,” tech. rep., 2010.

- [67] E. Arazo, D. Ortego, P. Albert, N. O’Connor, and K. McGuinness, “Unsupervised label noise modeling and loss correction,” in *ICML*, pp. 312–321, PMLR, 2019.
- [68] T. Chen, S. Kornblith, M. Norouzi, and G. Hinton, “A simple framework for contrastive learning of visual representations,” in *ICML*, pp. 1597–1607, PMLR, 2020.

Appendix for *Debiased Sample Selection for Combating Noisy Labels*

A ITEM with a Semi-Supervised Learning Framework

Considering the large scale of unreliable samples discarded, especially in considerable noise ratios, leveraging these samples through semi-supervised learning is necessary. Therefore, we provide a novel version of ITEM with stronger performance. The algorithm is shown in Algorithm 2. Besides, a strong augmentation CTAugment is used, which refers to [64]. Compared with its original version, the new training framework only adds two operations (shown in Lines 12 and 13). Thus, the code implementation is relatively convenient.

Algorithm 2 ITEM with a semi-supervised framework

Input: The training set D_N , training epoch T , warmup iterations T_w , a selection criterion $\text{Criterion}(\cdot)$, a classifier network with m experts, the mapping function $S^\beta(\cdot)$ with a hyperparameter β .

- 1: **Initialize** our network with one classifier layer and m expert layers $\mathbb{F} = \{f, g^1, \dots, g^m\}$.
 - 2: **for** $t = 1, \dots, T_w$ **do**
 - 3: Randomly sample f^c from \mathbb{F} , and WarmUp f^c on D_N .
 - 4: **end for**
 - 5: **for** $t = 1, \dots, T$ **do**
 - 6: Split D_N into the clean set \tilde{D}_{clean} and the unreliable set \tilde{D}_{noise} based on $\text{Criterion}(\mathbb{F})$, and discard labels in \tilde{D}_{noise} .
 - 7: Calculate weighted vector $\mathbf{v} = [\mathbf{w}_1, \dots, \mathbf{w}_K]$ on \tilde{D}_{clean} .
 - 8: Calculate reversed weighted vector $\tilde{\mathbf{v}} = [\tilde{\mathbf{w}}_1, \dots, \tilde{\mathbf{w}}_K]$ with Eq. (5).
 - 9: **while** $i = 1, \dots, \text{iterations}$ **do**
 - 10: Randomly sample a mini batch $B_v = \{(\mathbf{x}_i, \tilde{y}_i)\}_{i=1}^b$ from \tilde{D}_{clean} according to \mathbf{v} .
 - 11: Randomly sample a mini-batch $B_{\tilde{v}} = \{(\mathbf{x}'_i, \tilde{y}'_i)\}_{i=1}^b$ from \tilde{D}_{clean} according to $\tilde{\mathbf{v}}$.
 - 12: Draw a mini-batch $B = \{(\mathbf{x}''_i)\}_{i=1}^{2b}$ from \tilde{D}_{noise} without labels.
 - 13: Generate pseudo-labels, then have $B = \{(\mathbf{x}''_i, \tilde{y}''_i)\}_{i=1}^{2b}$, where $\tilde{y}''_i = \mathbb{E}_{f \sim \mathbb{F}}[f(\mathbf{x}''_i)]$.
 - 14: Randomly sample f^c from \mathbb{F} .
 - 15: Update network parameters via minimizing $\mathcal{L}(f^c(\text{MixUP}(B_v \text{ and } B_{\tilde{v}}, B)))$.
 - 16: **end while**
 - 17: **end for**
-

B More experimental results

B.1 Results on CIFAR-100N

We additionally verify the effectiveness of \ddagger ITEM on another human-annotated dataset, CIFAR-100N, whose noise ratio is roughly 40.2%. We adopt the same settings on CIFAR-100 (see Table 8), and the results are shown in Table 6. Our proposal ITEM achieves state-of-the-art performance on both supervised and semi-supervised frameworks.

B.2 Visualization

We verify the effectiveness of \ddagger ITEM on varying noisy conditions and show the following noise-robust results.

<i>w/o semi</i>		<i>w/ semi</i>	
CE	55.50 ± 0.66%	ELR +	66.72 ± 0.07%
Co-teaching	60.37 ± 0.27%	CORES*	55.72 ± 0.42%
SOP+	67.81 ± 0.23%	DivideMix	71.13 ± 0.48%
ITEM	69.47 ± 0.18%	ITEM*	72.40 ± 0.19%

Table 6: Test accuracy (%) on the test set of CIFAR-100N.

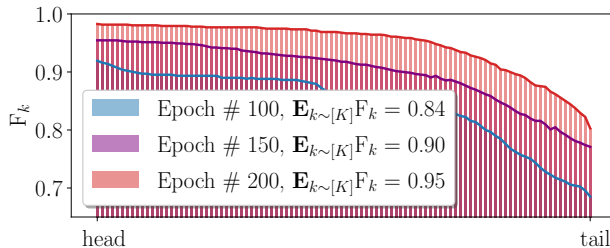


Figure 7: Visualization of class-level selection performance of ITEM on CIFAR-100 with 60% symmetric label noise. As the training process proceeds, ITEM gradually improves the F-score in all classes instead of only in head classes.

- **robust selection processes.** As shown in Figure 7, the total selection performance increases as the training progresses, while our framework has not degraded the selection performance on tail classes.
- **robust feature representations.** We visualize the learned representation of the test set on CIFAR-10. We compare three training manners and show the results in Figure 8. Compared with training on randomly sampled mini-batch and $B_{\bar{v}}$, our mixed sampling strategy yields a feature extractor with a strong representation. As shown in Figure 8c, the distance among varying class clusters is closer, reflecting that the classifier learns more robust decision boundaries.
- **robust training curves.** We conduct ablation studies to verify the effectiveness of our proposed robust network architecture. The results on two noisy settings are shown in Figure 9. We can see that compared with a single network (a normal ResNet structure), our expert network achieves more robustness. Meanwhile, the mixed sampling strategy also contributes to improving generalization performance.

B.3 Results on Fine-Grained Noisy Settings

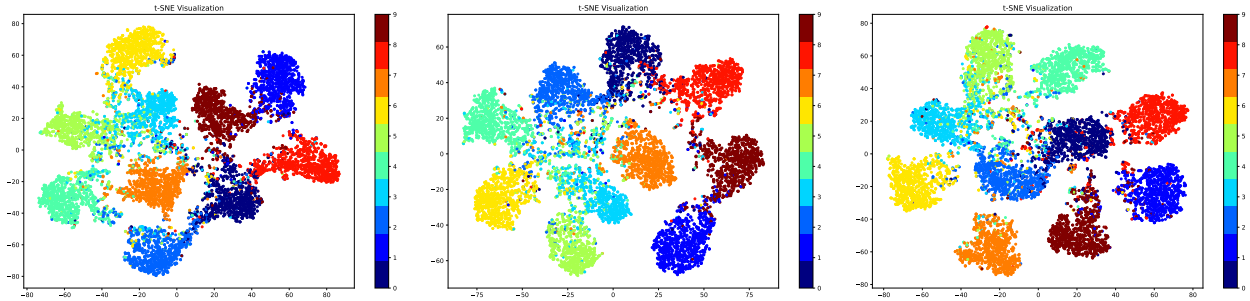
The literature [5] pointed out that noisy label’ generation is strongly associated with fine-grained datasets. Following settings in SNSCL [5], we conduct experiments on four noisy fine-grained datasets, including Stanford Dogs [65] and CUB-200-2011 [66]. A ResNet-18 pre-trained on ImageNet with three experts ($m = 3$) is utilized. We synthetically construct two noise types, symmetric and asymmetric noise labels.

The results are shown in Table 7. Our method achieves significant generalization performance even when tackling fine-grained noisy classification and consistently outperforms other methods by a large margin. We consider the MixUp operation to be the primary contribution to the advanced performance on fine-grained datasets since it encourages the model to learn from structured data instead of the unstructured noise [67].

C Experimental Settings

We reported the statistical data of four datasets and the whole experimental setup in Table 8. Besides, the data augmentation strategy for different datasets can be divided into two parts.

- For CIFAR-10, CIFAR-100, and CIFAR-10N, randomly cropping and horizontally flipping are adopted.



(a) Training on randomly sampled mini-batch B , the best test accuracy is 88.42%. (b) Training on B_v only, the best test accuracy is 90.17%. (c) Training on $\text{MixUP}(B_v, B_{\bar{v}})$, the best test accuracy is 93.04%.

Figure 8: Visualizing feature representations on the CIFAR-10 test set by T-SNE. The noise setting is 40% symmetric noisy labels.

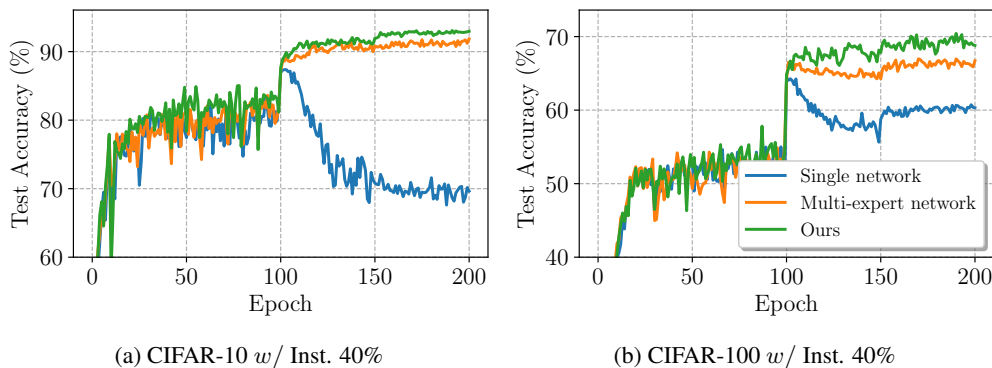


Figure 9: Visualization of training curves under three settings. Suppose a *small-loss* criterion with the loss threshold, we compare our methods (Ours) with the proposed multi-expert network and single network on two noise conditions.

- For Clothing-1M, we first resize the image to 256x256 and then randomly crop it to 224x224. Besides, the horizontally flipping is adopted.

Meanwhile, we detailedly exhibit the noise generation process by the noise transition matrix. As shown in Figure 10, given a noise ratio ρ , the noise transition matrix T is represented as $T_{ij}(\mathbf{x}) = P(\tilde{y} = j | y = i)$, where T_{ij} denotes that the label of the instance transits from a clean label i to a noisy label j . The generation process of instance-dependent label noise can be found in the work [11, 23].

C.1 Settings for Learning with Noisy Labels on Imbalanced Datasets

We obey the same manner of imbalanced noise construction from RCAL [62] and conduct experiments on synthetic CIFAR-10 and CIFAR-100. Concretely, we set the batch size as 64 and run 200 epochs for both CIFAR-10 and CIFAR-100. The learning rate is set as 0.02 and reduced by a factor of 10 at {100, 150}-th epoch. A ResNet-32 network with 4 experts is utilized. Besides, for a fair comparison, we adopt the same augmentation policy SimAug [68] as RCAL.

Methods	Stanford Dogs		CUB-200-2011		Avg
	Sym 40%	Asy 30%	Sym 40%	Asy 30%	
CE	51.42	58.08	64.01	56.02	57.38
Label Smooth	70.22	<u>64.99</u>	54.39	56.80	61.60
Conf. Penalty	68.69	64.50	52.40	54.33	59.98
Co-teaching	49.15	50.50	46.57	50.60	49.21
JoCoR	49.62	53.59	52.64	51.70	51.89
CE + SNSCL	75.27	64.49	<u>68.83</u>	<u>61.48</u>	<u>67.52</u>
‡ ITEM	<u>74.92</u>	68.19	70.04	66.58	69.93

Table 7: Test accuracy (%) on two fine-grained benchmarks with two noisy settings. The best and the second best performances are highlighted with **Bold** and underline, respectively.

Table 8: Detailed settings about training procedure of *ITEM*.

	CIFAR-10	CIFAR-100	CIFAR-10N (all conditions)	Clothing-1M
Statistic data				
Class number	10	10	10	14
Training size	50,000	50,000	50,000	1,000,000
Testing size	10,000	10,000	10,000	10,000
Training procedure				
Network	ResNet-18	ResNet-34		Pre-trained ResNet-50
Batch size	64			100
Epoch	200			10
Warmup epoch	10	30	10	1
Optimizer	SGD			
Momentum	0.9			
Learning rate (LR)	0.02			0.001
Weight decay	1e-3			5e-4
LR scheduler	divided by 10 at [100,150]-th epoch			divided by 10 at 5-th epoch
Hyperparameters				
the num. of experts m	$m = 4$			$m = 2$
the slope parameter β	$\beta = 3$			

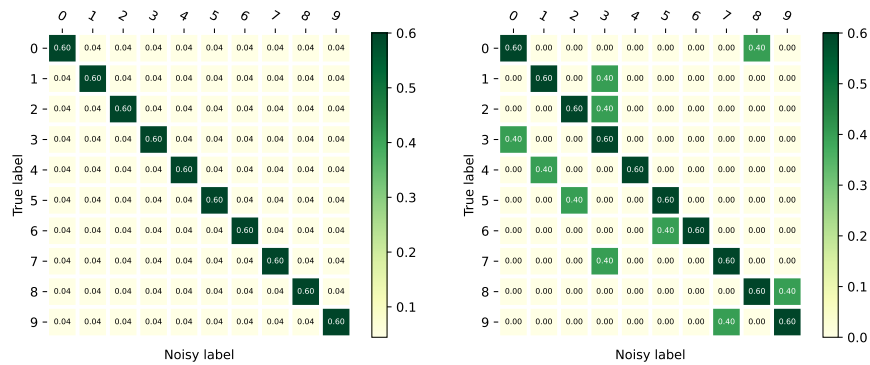


Figure 10: Visualization of the transition matrix for symmetric (left) and asymmetric (right) noise on a ten classification task when the noise ratio is 40%.